Computers and Structures 323 (2026) 108164

Contents lists available at ScienceDirect

Computers and Structures

journal homepage: www.elsevier.com/locate/cas

Stochastic seakeeping analysis of nonlinear ship rolling dynamics under non-stationary and irregular sea states

Ioannis P. Mitseas*, Omar Danisworo

School of Civil Engineering, University of Leeds, Leeds, LS2 9JT, UK

ARTICLE INFO

Keywords:
Ship rolling dynamics
Stochastic averaging
Seakeeping probability
Sea-wave power spectra
Negative stiffness
Statistical linearization

ABSTRACT

This paper presents an efficient semi-analytical methodology for quantifying the capsizing risk and seakeeping performance of ships undergoing nonlinear rolling motions under realistic, non-white sea-wave excitations. The dynamic response is captured through a comprehensive and physically consistent nonlinear formulation that incorporates both softening and hardening restoring moment characteristics, nonlinear hydrodynamic damping mechanisms, and evolutionary stochastic wave loads representative of complex maritime environments. By leveraging a refined blend of stochastic averaging and statistical linearization techniques, the study yields computationally efficient, time-dependent seakeeping probability estimates, rigorously accounting for the critical behaviors of both bounded and unbounded ship roll motions, including those associated with negative stiffness regions, through an appropriately tailored, non-stationary response amplitude probability density function (PDF). A notable advancement of the proposed framework lies in its robust capability to address stochastic sea-wave excitations with time-varying intensity and frequency content, thereby accurately reflecting the evolving nature of real-world open-sea environments. Numerical analyses across a range of case studies, validated against benchmark Monte Carlo simulations, demonstrate the accuracy and efficiency of the methodology, underscoring its promise as a practical performance-based tool for evaluating vessel stability and seakeeping under dynamic and uncertain maritime operational scenarios.

1. Introduction

The stability of marine vessels remains a cornerstone of naval architecture, directly impacting both operational safety and design efficacy. Traditional stability assessment has largely relied on static and quasi-static criteria, which, while foundational, are inadequate to capture the complex ship dynamic behaviors under the intricate and highly dynamic loading conditions encountered in open seas. Contemporary maritime operations routinely expose vessels to irregular, large-amplitude wave actions and complex environmental uncertainties, highlighting the critical limitations of conventional hydrostatic analyses. These shortcomings have catalyzed a pronounced shift within the field toward probabilistic and dynamics-based frameworks, with growing emphasis on time-dependent responses and rare-event phenomena such as capsizing. Within this evolving context, the characterization and quantification of ship roll dynamics under stochastic sea-wave excitations have garnered significant attention. Large-amplitude rolling, particularly in beam seas, poses acute risks for vessel safety and performance (e.g., [1–5]). The transient and nonlinear nature of these motions, compounded by the non-white, non-stationary properties of ocean wave fields, presents formidable challenges for both theoretical modeling and practical reliability assessment. To advance safety margins and support robust design, there is an urgent need for analytical and computational tools that not only describe ship motion in adverse open sea conditions but also quantify the associated risks within a reliability-informed framework (e.g., [6–9]). Recent advances have sought to bridge these gaps through the integration of high-fidelity nonlinear models and stochastic process theory. Comprehensive representations of ship roll dynamics, incorporating both softening and hardening restoring characteristics as well as nonlinear hydrodynamic damping, are now recognized as essential for capturing the full spectrum of possible roll behaviors. In pursuit of physical relevance and consistency with current standards, the adoption of a JONSWAP-type sea spectrum for wave excitation modeling is among the approaches endorsed in contemporary offshore and maritime design codes (e.g., [10,11]).

Despite ongoing improvements in design practices and safety regulations, ship capsizing incidents persist, often resulting in substantial

* Corresponding author.
Email address: I.Mitseas@leeds.ac.uk (I.P. Mitseas).

https://doi.org/10.1016/j.compstruc.2026.108164
Received 7 November 2025; Accepted 19 February 2026
Available online 25 February 2026

losses of vessels, cargo, and human life (e.g., [6,12]). Such catastrophic events are typically precipitated by rare but critical dynamic responses that breach established stability thresholds, rendering them particularly amenable to investigation through the lens of the first-passage problem (e.g., [7,12–14]). In this context, capsize likelihood is formally characterized as the probability that the ship rolling response first exceeds a prescribed critical rotation angle under evolutionary stochastic excitation, given that no prior exceedance has occurred. This approach yields a rigorous and quantifiable metric for assessing vessel seakeeping ability. Advanced Monte Carlo simulation (MCS) techniques have become a standard tool for estimating the probability of such critical events within reliability analysis (e.g., Schueller et al. [15]). Nevertheless, for complex nonlinear models (e.g., [16–18]) subjected to evolutionary stochastic excitation, the computational cost of MCS can be prohibitive, particularly when higher-order statistical descriptors such as response probability density functions (PDFs) are required. This difficulty is further compounded by the inherent rarity of capsizing events involving undamaged ships operating under normal conditions. As noted in Ref. [19], capturing such rare occurrences through direct time-domain numerical simulation demands an exceptionally large number of realizations. The computational burden associated with producing these datasets using high-fidelity engineering models is typically prohibitive. This challenge motivates the development of efficient approximate analytical methods (e.g., Barbato and Conte [20]), frameworks related to modeling the response as a one-dimensional Markov process (e.g., [21–23]), probability density evolution schemes (e.g., [24–26]), and stochastic averaging/linearization techniques (e.g., [27–32]).

Several notable studies have addressed the first-passage problem in the context of ship dynamics. To and Chen [7] proposed the Generalized Extended Stochastic Central Difference (GESCD) method, a semi-analytical technique designed to efficiently approximate first-passage probabilities in nonlinear ship rolling under non-stationary narrow-band excitations, showing very good agreement with MCS data. Moshchuk et al. [33] employed an asymptotic expansion technique to solve Pontryagin's partial differential equation for mean exit times, offering analytical insight into the role of energy levels and excitation characteristics in capsizing risk. Kougioumtzoglou and Spanos [12] developed a numerical path integral scheme for deriving non-stationary first-passage PDFs of nonlinear roll dynamics, demonstrating its effectiveness in capturing extreme ship responses when benchmarked against MCS results. Ren et al. [34] advanced a path integration approach incorporating inelastic impacts and non-smooth transformations to analyze first-passage probabilities in icy sea environments, broadening applicability to harsh maritime conditions.

Fig. 1 illustrates the dynamic evolution of ship roll motion, progressing from small angles near the upright stable equilibrium to large-amplitude rolling that can culminate in capsize and loss of stability. The inherently nonlinear character of ship rolling presents significant modeling challenges (e.g., Malara et al. [35]), particularly in capturing the complex dynamics associated with large-amplitude motions and potential capsize events. Among the modeling approaches, the softening Duffing oscillator has gained considerable traction in the field of ship dynamics, providing a satisfactory approximation of the restoring moment through a linear-plus-cubic formulation (e.g., [2,3,12,22,23]). While such models are often phenomenological, they manage to replicate basic aspects of the ship roll response.

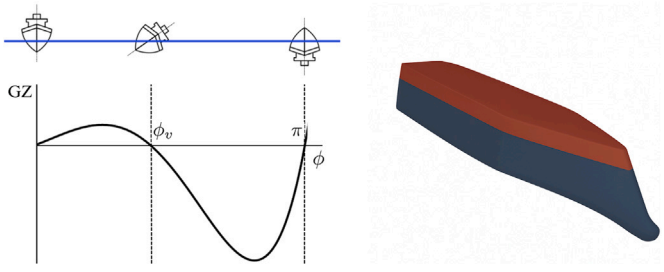

Fig. 1. Transition from near-upright ship rolling to large-amplitude motions leading to the capsized equilibrium position. Phase plane topology of capsizing in ship dynamics.

This research contributes a refined semi-analytical methodology for the time-dependent assessment of ship seakeeping ability and capsizing risk under realistic, evolutionary sea-wave excitations. The central innovation lies in the seamless integration of stochastic averaging and statistical linearization techniques with comprehensive nonlinear ship roll modeling, providing a robust and computationally efficient platform for evaluating vessel performance in non-stationary and irregular sea states. A key advancement of this framework is its ability to rigorously account for both bounded and unbounded motions by explicitly incorporating the critical effects of negative stiffness, phenomena often simplified in conventional models. By capturing the evolving statistical properties of the response amplitude, the method achieves significant computational savings compared to exhaustive Monte Carlo simulations while maintaining adequate levels of accuracy. Extensive validation against benchmark simulations underscores the utility and applicability of the proposed technique for modern naval engineering practice. To enhance physical fidelity, the proposed methodology utilizes sophisticated nonlinear formulations, including higher-order odd-degree polynomial representations of the restoring moment, which are shown to effectively capture the essential nonlinear behaviors of ships in beam sea-wave excitations (e.g., Taylan [36]). These formulations enable the modeling of key physical phenomena such as restoring asymmetry, softening and hardening effects, and progressive loss of stiffness at high roll angles. In particular, the righting lever (GZ) curve is represented as a fifth-order polynomial, striking a balance between physical realism and analytical tractability, and is coupled with evolutionary stochastic sea-wave excitation models consistent with modern maritime design codes. Nonlinear hydrodynamic damping effects are also incorporated to limit large roll amplitudes and accurately model energy dissipation mechanisms (e.g., [2,35,36]). Lastly, the method rigorously captures both bounded and unbounded dynamic rolling by introducing a tailored form of the non-stationary response amplitude PDF, designed to capture the probabilistic signatures of nonlinear ship roll dynamics, including those associated with negative-stiffness effects.

The remainder of the paper is organized as follows. Sections 2.1–2.4 present the mathematical foundations underpinning the developed stochastic dynamics vessel seakeeping assessment framework. Section 2.5 provides insights into the key characteristics and practical implications of the methodology. Section 3 illustrates the application of the framework through representative case studies in marine engineering. The accuracy of the proposed technique is evaluated by comparing the derived results with pertinent MCS data obtained from nonlinear ship rolling time-history analysis (RHA). Finally, Section 4 summarizes the main findings and conclusions of the study.

2. Mathematical formulation

This section outlines the mathematical foundations underlying the proposed efficient stochastic dynamics seakeeping assessment methodology. Emphasis is placed on the modeling assumptions and simplifications introduced to facilitate numerical efficiency, while maintaining consistency with the adopted complex nonlinear governing equation for ship rolling motion.

2.1. Sea-wave evolutionary excitation spectrum

The induced sea-wave excitation is modeled as a zero-mean Gaussian nonstationary stochastic process characterized by an evolutionary power spectrum (EPS). This modeling approach captures the time-varying distribution of energy in the roll-moment excitation spectrum and is

defined as

$$S_w(\omega,t) = |g(t)|^2 |F_{\text{roll}}(\omega)|^2 S_{\text{JS}}(\omega, H_s, T_p) \tag{1}$$

where $S_{\text{JS}}(\omega)$ denotes the stationary JONSWAP wave–energy spectrum, $F_{\text{roll}}(\omega)$ is a frequency-dependent transfer function that maps wave energy into roll-moment excitation (e.g., Jiang et al. [37]), and $g(t)$ is a time envelope function that introduces nonstationarity into the process. Particular attention is given to the JONSWAP model [38], which following the IEC 61,400–3 guidelines [11], produces a narrow-banded spectrum with a pronounced peak at the dominant wave frequency. The inclusion of the function $F_{\text{roll}}(\omega)$, however, has been shown to broaden the excitation spectrum. Subsequently, the adopted JONSWAP spectrum takes the form

$$S_{JS}(\omega, H_s, T_p,) = 0.3125 T_p H_s^2 \left(\frac{\omega}{\omega_p}\right)^{-5} \exp\left[-1.25\left(\frac{\omega}{\omega_p}\right)^{-4}\right] M(\omega) \tag{2}$$

where $\omega_p = 2\pi/T_p$ is the peak frequency, and the term $M(\omega)$ defines the spectral peak enhancement

$$M(\omega) = (1 - 0.287\log\gamma)\gamma^{\exp\left[-0.5\left(\frac{\omega/\omega_p - 1}{\sigma}\right)^2\right]} \tag{3}$$

In line with IEC 61400–3 (e.g., [11,39]) and established practice, the peak-shape parameter is set to $\gamma = 3.3$, with $\sigma = 0.07$ for frequencies below the peak frequency ω_p and $\sigma = 0.09$ otherwise. The function F_{roll}, is defined as $|F_{\text{roll}}|^2 = C\omega^4$ with $C = 3$ reflecting beam-sea loading conditions and system properties. To model non-stationarity, the time envelope function $g(t)$ is adopted in the form

$$g(t) = \left\{0.2 + 0.8 \times \left[\frac{t}{a}\exp\left(1 - \frac{t}{a}\right)\right]^b\right\}^{0.5} \tag{4}$$

where the shaping parameters are chosen as $a = 20$ and $b = 5$ governing the growth and decay characteristics of the envelope function. The peak period T_p and significant wave height H_s are defined in the numerical application section. For demonstration purposes, a couple of resulting EPS are shown in Fig. 2, where the characteristic narrow-band peak trend of the JONSWAP spectrum is observed. The broadening of the high-frequency tail is attributed to the inclusion of the F_{roll} function, which introduces additional energy into the higher-frequency range of the excitation profile.

2.2. Nonlinear ship rolling dynamics modeling

The ship rolling under stochastic sea-wave excitation is governed by a second-order differential equation featuring linear and nonlinear hydrodynamic damping terms, along with a nonlinear restoring moment. While the restoring moment is commonly approximated using odd-order polynomials, hydrodynamic damping formulations vary widely across the literature (e.g., [27,35,36,40,41]). In the present study, a formulation proposed by Taylan is adopted, in which the roll motion is modeled using a quintic polynomial representation for the righting arm (GZ) curve, combined with a B1-type hydrodynamic damping scheme as appears in [36]. The governing dynamics of the nonlinear ship rolling equation are expressed as

$$(I_{xx} + \delta I_{xx})\ddot{\phi}(t) + B_L\dot{\phi}(t) + B_N\dot{\phi}(t)|\dot{\phi}(t)| + \Delta(C_1\phi(t) + C_3\phi^3(t) + C_5\phi^5(t)) = I_{xx}w(t) \tag{5}$$

Here, $\phi(t)$ is the roll angle, I_{xx} is the ship roll moment of inertia, δI_{xx} is the added moment of inertia in roll, $w(t)$ represents the Gaussian zero-mean non-stationary stochastic process possessing the evolutionary power spectrum in the form of Eq. (1), Δ is the weight displacement, and B_L and B_N are the linear and nonlinear damping coefficients, respectively. Note that the squared velocity term is expressed as $\dot{\phi}(t)|\dot{\phi}(t)|$, ensuring that the damping force always opposes the motion. This formulation guarantees that, regardless of the sign of $\dot{\phi}(t)$, the damping moment remains directed opposite to the roll velocity, thereby accurately modeling energy dissipation due to nonlinear hydrodynamic effects. The coefficients C_1, C_3, C_5 correspond to the linear, cubic, and quintic terms of the restoring moment, derived from the ship GZ curve. These are defined as

$$C_1 = \frac{d(GZ)}{d\phi} = GM \tag{6}$$

$$C_3 = \frac{4}{\phi_v^4}\left(3A_{\phi v} - GM\phi_v^2\right) \tag{7}$$

$$C_5 = -\frac{3}{\phi_v^6}\left(4A_{\phi v} - GM\phi_v^2\right) \tag{8}$$

In these expressions, GM denotes the metacentric height, ϕ_v is the vanishing stability angle, and $A_{\phi v}$ is the area under the GZ curve. By dividing

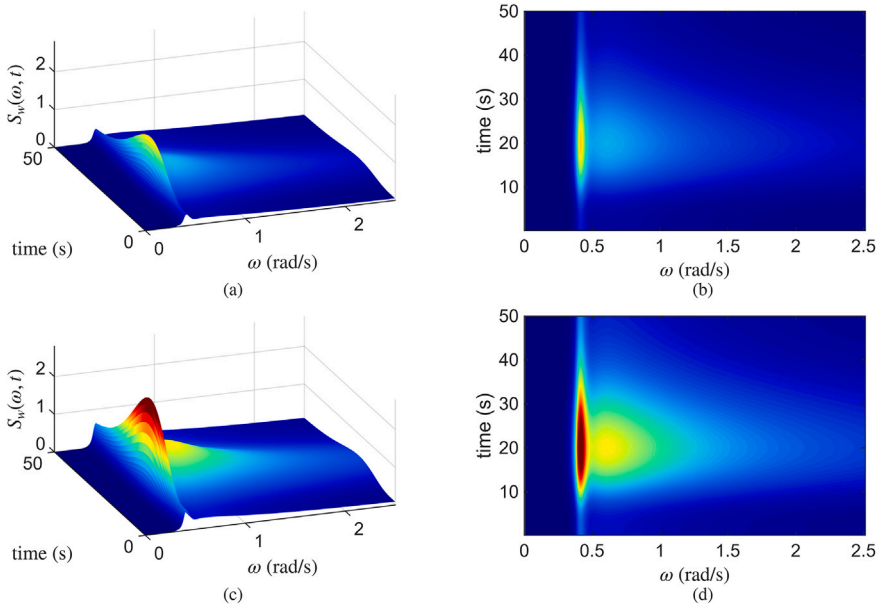

Fig. 2. Evolutionary roll moment excitation spectra $S_w(\omega,t)$ for peak period $T_p = 15.5$ s and different values of significant wave height: (a), (b) correspond to $H_s = 6$ m; (c), (d) correspond to $H_s = 8$ m.

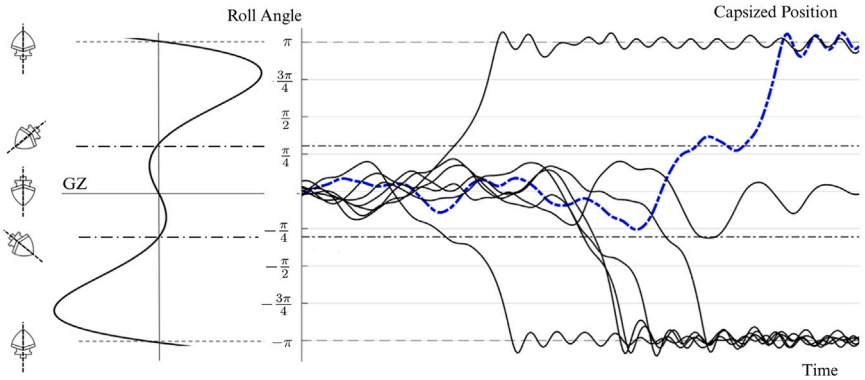

Fig. 3. Ship rolling time-histories under stochastic sea-wave excitation, illustrating a potential capsizing event for $\phi > \phi_v$ when $\phi > 0$ and $\phi < \phi_v$ when $\phi < 0$. Also depicted is the roll restoring arm (GZ) curve, characteristic of nonlinear ship dynamics.

through $I_{xx}+\delta I_{xx}$ and substituting the C_1, C_3, C_5, Eq. (5) is reformulated to emphasize the role of nonlinear contributions in the ensuing seakeeping analysis. The nonlinear components are each scaled by distinct weighting factors ε_1, ε_2, and ε_3, yielding the final form

$$\ddot{\phi}(t)+b_L\dot{\phi}(t)+\varepsilon_1 b_N\dot{\phi}(t)|\dot{\phi}(t)|+\omega_\phi^2\phi(t)+\varepsilon_2 m_3\phi^3(t)+\varepsilon_3 m_5\phi^5(t)=\lambda w(t) \quad (9)$$

where the normalized coefficients are given by

$$\omega_\phi^2=\frac{\Delta GM}{I_{xx}+\delta I_{xx}} \quad (10)$$

$$m_3=\frac{4\omega_\phi^2}{\phi_v^2}\left(\frac{3A_{\phi_v}}{GM\phi_v^2}-1\right) \quad (11)$$

$$m_5=-\frac{3\omega_\phi^2}{\phi_v^4}\left(\frac{4A_{\phi v}}{GM\phi_v^2}-1\right) \quad (12)$$

$$b_L=\frac{B_L}{I_{xx}+\delta I_{xx}} \quad (13)$$

$$b_N=\frac{B_N}{I_{xx}+\delta I_{xx}} \quad (14)$$

and the nondimensional inertia term $\lambda=\frac{I_{xx}}{I_{xx}+\delta I_{xx}}$. The weighting factors introduce modeling flexibility by enabling the representation of physically meaningful hydrodynamic damping and restoring behaviors. They enhance adaptability, allowing the model to capture a wide range of ship-specific dynamic responses and design requirements.

Fig. 3 illustrates a set of ship rolling response time histories under stochastic sea-wave excitation, plotted alongside the roll restoring lever (GZ) curve. The GZ curve, located on the left, represents the vessel's restoring behavior, with a characteristic angle of vanishing stability ϕ_v beyond which the stability becomes questionable. On the right, several sample response trajectories are presented, with the blue dashed line representing a notable case. In this specific trajectory, the roll response exceeds the angle of vanishing stability ϕ_v indicating a temporary loss of stability. However, due to the presence of a hardening effect in the restoring moment, the vessel avoids an immediate transition into the capsized state. Instead, it temporarily re-stabilizes before eventually capsizing at a later time. This demonstrates that exceeding the angle of vanishing stability does not inevitably lead to capsizing, particularly when higher-order restoring characteristics (e.g., a positive fifth-order stiffness term) provide sufficient restoring moment to resist rollover. The figure highlights the nuanced interplay between nonlinear restoring forces and excitation variability in governing ship stability.

2.3. Statistical linearization and stochastic averaging treatment

Having defined both the excitation stochastic process and the nonlinear roll motion equation, this subsection focuses on the response dynamic analysis; see also [13,42]. The approach relies on a stochastic averaging treatment applied to the system dynamics, reducing the original nonlinear second-order differential equation to a first-order stochastic differential equation (SDE) governing the evolution of the roll angle amplitude. Assuming the system of Eq. (9) is lightly damped and excited by Eq. (1), it is expected to exhibit a pseudo-harmonic behavior under non-capsizing conditions, characterized by a slowly varying with time roll angle amplitude $A(t)$ and a slowly varying with time phase $\phi(t)$. Therefore, the roll angle satisfies

$$\phi(t)=A(t)\cos(\psi), \quad \dot{\phi}(t)=-\omega(A)A(t)\sin(\psi) \quad (15)$$

with ψ defined as:

$$\psi=\omega(A)t+\theta(t) \quad (16)$$

Here, $A(t)$ and $\theta(t)$ denote slowly time-varying functions, treated as constants over a single oscillation cycle. This enables the use of equivalent linearization (e.g., Roberts and Spanos [43]), transforming Eq. (9) into

$$\ddot{\phi}(t)+\beta(A)\dot{\phi}(t)+\omega^2(A)\phi(t)=\lambda w(t) \quad (17)$$

The equivalent amplitude-dependent hydrodynamic damping $\beta(A)$ and stiffness elements $\omega(A)$ are defined as

$$\beta(A)=b_L+\frac{S(A)}{A\omega(A)} \quad (18)$$

and

$$\omega^2(A)=\frac{C(A)}{A} \quad (19)$$

with

$$S(A)=-\frac{1}{\pi}\int_0^{2\pi}\sin\psi\Big(-\varepsilon_1 b_N\omega(A)A\sin\psi\cdot|-\omega(A)A\sin\psi| +\omega_\phi^2 A\cos\psi+\varepsilon_2 m_3(A\cos\psi)^3+\varepsilon_3 m_5(A\cos\psi)^5\Big)\,d\psi \quad (20)$$

and

$$C(A)=\frac{1}{\pi}\int_0^{2\pi}\cos\psi\Big(-\varepsilon_1 b_N\omega(A)A\sin\psi\cdot|-\omega(A)A\sin\psi| +\omega_\phi^2 A\cos\psi+\varepsilon_2 m_3(A\cos\psi)^3+\varepsilon_3 m_5(A\cos\psi)^5\Big)\,d\psi \quad (21)$$

By substituting Eqs. (20) and (21) into Eqs. (18) and (19), respectively, the analytical expressions for the amplitude-dependent equivalent elements are obtained in the following form

$$\beta(A) = b_L + \frac{8}{3\pi} b_N \omega(A) A \tag{22}$$

and

$$\omega^2(A) = \omega_\phi^2 + \frac{3}{4} A^2 m_3 + \frac{5}{8} A^4 m_5 \tag{23}$$

A tailored form for the non-stationary roll angle amplitude PDF $p(A,t)$ is proposed (e.g., Kougioumtzoglou et al. [27])

$$p(A,t) = \frac{A}{c(t)} \exp\left(-\frac{A^2}{2c(t)}\right) \mathrm{rect}(A) + \exp\left(-\frac{A_{cr}^2}{2c(t)}\right) \delta(A - A_\infty) \tag{24}$$

where $\mathrm{rect}(A) = u(A) - u(A - A_{cr})$, with $u(\cdot)$ denoting the unit step function, $c(t)$ is a coefficient to be determined, and $\delta(\cdot)$ is the Dirac delta function. Next, based on Eq. (24), an alternative equivalent linear system to Eq. (17) can be introduced as

$$\ddot{\phi}(t) + \beta_{\mathrm{eq}}(t)\dot{\phi}(t) + \omega_{\mathrm{eq}}^2(t)\phi(t) = \lambda w(t) \tag{25}$$

featuring time-varying equivalent elements of the form (e.g., Kougioumtzoglou et al. [27])

$$\beta_{\mathrm{eq}}(t) = b_L + \int_0^\infty \frac{S(A)}{A\omega(A)} p(A,t)\,\mathrm{d}A \tag{26}$$

and

$$\omega_{\mathrm{eq}}^2(t) = \int_0^\infty \frac{C(A)}{A} p(A,t)\,\mathrm{d}A \tag{27}$$

Relying on the nature of the roll angle amplitude PDF $p(A,t)$, the time-varying equivalent elements include two parts; the bounded, for $A \in [0, A_{cr}]$, and the unbounded part for $A \in (A_{cr}, \infty)$, which may lead to capsizing. Within this framework, the bounded equivalent stiffness $\omega_{eq,B}^2(t)$ element is given by

$$\omega_{eq,B}^2(t) = \int_0^{A_{cr}} \frac{C(A)}{A} p(A,t)\,\mathrm{d}A \tag{28}$$

While the corresponding bounded equivalent hydrodynamic damping $\beta_{eq,B}(t)$ element reads

$$\beta_{eq,B}(t) = b_L + \int_0^{A_{cr}} \frac{S(A)}{A\omega(A)} p(A,t)\,\mathrm{d}A \tag{29}$$

The evaluation of the seakeeping probability requires the definition of a critical rolling amplitude A_{cr}. In this study, the following criterion is adopted: $\omega^2(A_{\mathrm{cr}}) = 0$. Notably, capsizing is considered to occur when the roll angle amplitude A exceeds this critical threshold A_{cr}, resulting in negative values of the resulting stiffness component, which further promotes capsizing. Elaborating on Eqs. (28) and (29) yields

$$\omega_{\mathrm{eq,B}}^2(t) = \omega_\phi^2 + \frac{3}{2}\varepsilon_2 c(t) m_3 + 5\varepsilon_3 c^2(t) m_5 - \frac{A_{\mathrm{cr}}^2\left(5\varepsilon_3 m_5 A_{\mathrm{cr}}^2 + 6\varepsilon_2 m_3 + 20\varepsilon_3 c(t) m_5\right)}{8\left(S(t) - 1\right)} \tag{30}$$

and

$$\beta_{\mathrm{eq,B}}(t) = b_L + \int_0^{A_{\mathrm{cr}}} \frac{8}{3\pi}\varepsilon_1 b_N A\left(\omega_\phi^2 + \frac{3}{4}\varepsilon_2 A^2 m_3 + \frac{5}{8}\varepsilon_3 A^4 m_5\right)^{1/2} p(A,t)\,\mathrm{d}A \tag{31}$$

where the time-varying factor $S(t)$ is determined by applying the normalization condition $\int_0^\infty p(A,t) = 1$, and yields $S(t) = \exp[-A_{cr}^2/(2c(t))]$.

A combination of deterministic and stochastic averaging (e.g., Mitseas and Beer [13]) yields a first-order SDE governing the evolution of roll angle amplitude

$$\dot{A}(t) = -\frac{1}{2}\beta_{\mathrm{eq,B}}(t)A(t) + \frac{\pi\lambda^2 S_w(\omega_{\mathrm{eq,B}}(t),t)}{2A(t)\omega_{\mathrm{eq,B}}^2(t)} + \frac{\left[\pi S_w(\omega_{\mathrm{eq,B}}(t),t)\right]^{1/2}}{\omega_{\mathrm{eq,B}}(t)}\lambda\eta(t) \tag{32}$$

where $\eta(t)$ is a zero-mean and delta-correlated process of unit intensity, with $E(\eta(t)) = 0$; and $E(\eta(t)\eta(t+\tau)) = \delta(t)$ (e.g., [42,44,45]). Eq. (32) signifies that the amplitude process $A(t)$ is decoupled from the phase $\phi(t)$ and, thus, can be modeled as a one-dimensional Markov process, enabling the formulation of a Fokker-Planck equation that governs the associated transition response amplitude PDF (e.g., [46,47])

$$\frac{\partial p(A,t|A_1,t_1)}{\partial t} = -\frac{\partial}{\partial A}\left\{\left(-\frac{\beta_{\mathrm{eq,B}}(t)}{2}A + \frac{\pi\lambda^2 S_w(\omega_{\mathrm{eq,B}}(t),t)}{2A\omega_{\mathrm{eq,B}}^2(t)}\right)p(A,t|A_1,t_1)\right\} + \frac{\pi\lambda^2 S_w(\omega_{\mathrm{eq,B}}(t),t)}{2\omega_{\mathrm{eq,B}}^2(t)}\frac{\partial^2 p(A,t|A_1,t_1)}{\partial A^2}. \tag{33}$$

Substituting the truncated Rayleigh PDF of Eq. (24) into Eq. (33) under the condition that A_1 and t_1 are zero-valued, the following nonlinear differential equation can be obtained for the computation of the time-varying coefficient $c(t)$:

$$\dot{c}(t) = -\beta_{\mathrm{eq,B}}(t)\,c(t) + \frac{\pi\,\lambda^2 S_w(\omega_{\mathrm{eq,B}}(t),t)}{\omega_{\mathrm{eq,B}}^2(t)} \tag{34}$$

Next, the transition amplitude PDF $p(a,t|a_1,t_1)$ can be derived in the form (e.g., Spanos and Solomos [46])

$$p(A,t|A_1,t_1) = \begin{cases} p_{\mathrm{tr}}(A,t|A_1,t_1) + R(t,t_1)\delta(A - A_\infty), & 0 < A_1 < A_{cr} \\ \delta(A - A_\infty), & A_1 > A_{cr} \end{cases} \tag{35}$$

with

$$p_{tr}(A,t \mid A_1,t_1) = \frac{A}{c(t,t_1)}\exp\left[-\frac{A^2 + h^2(t,t_1)}{2c(t,t_1)}\right] I_0\left(\frac{Ah(t,t_1)}{c(t,t_1)}\right)\mathrm{rect}(A) \tag{36}$$

where $I_0(.)$ denotes the modified Bessel function of the first kind and zero order with $c(t,t_1)$ and $h(t,t_1)$ being time-varying coefficients to be solved. Similar to the derivation of Eq. (34), substitution of the bounded part of Eq. (35) into Eq. (33), with the condition that $A \in [0, A_{cr}]$ and $A_1 \in [0, A_{cr}]$, yields the first-order differential equations of the time-varying coefficients

$$\frac{dc(t,t_1)}{dt} + \beta_{\mathrm{eq,B}}(t)c(t,t_1) - \frac{\pi\lambda^2 S_w(\omega_{\mathrm{eq,B}}(t),t)}{\omega_{\mathrm{eq,B}}^2(t)} = 0 \tag{37}$$

and

$$\frac{dh(t,t_1)}{dt} + \frac{\beta_{\mathrm{eq,B}}(t)}{2}h(t,t_1) = 0 \tag{38}$$

where Eqs. (37) and (38) are subjected to the initial condition $p(A,t|A_1,t_1) = \delta(A - A_1)$, meaning that no change of state occurs if the transition time is zero. Additionally, applying the normalization condition of the PDF $\int_0^\infty p_{tr}(A,t|A_1,t_1)dA = 1$ yields the time-varying coefficient

$$R(t,t_1) = 1 - \int_0^{A_{cr}} p_{tr}(A,t|A_1,t_1)dA \tag{39}$$

2.4. Seakeeping probability assessment and capsizing risk

In this section, the seakeeping probability pertaining to a ship rolling in open sea conditions is considered. The seakeeping probability in this case is defined as the probability $P_S(t)$ that the rolling amplitude A is kept below the specified threshold A_{cr} over the time duration $[0, T]$. In order to facilitate the numerical implementation, an adaptive discretization scheme is employed by dividing time into intervals (e.g., [13,27])

$$[t_{i-1}, t_i], \quad i = 1, 2, \dots, M, \quad t_0 = 0, \quad t_M = T, \quad \text{and}$$
$$t_i = t_{i-1} + d_T T_{\text{eq}}(t_{i-1}) \tag{40}$$

where T_{eq} is the equivalent natural period of the ship rolling system $T_{\text{eq}}(t) = \frac{2\pi}{\omega_{\text{eq}}(t)}$ and d_T is a constant in $(0, 1]$. Next, the seakeeping probability $P_S(t)$ is computed via

$$P_S(T = t_M) = \prod_{i=1}^{M} (1 - P_{Ci}) \tag{41}$$

with P_{Ci} defined as the capsizing probability of the first-passage kind, representing the likelihood that the roll angle amplitude exceeds the critical threshold A_{cr} within the time interval $[t_{i-1}, t_i]$, given that no such exceedance has occurred before t_{i-1}

$$P_{Ci} = \frac{\text{Prob}[A(t_i) \geq A_{cr} \cap A(t_{i-1}) < A_{cr}]}{\text{Prob}[A(t_{i-1}) < A_{cr}]} = \frac{Q_{i-1,i}}{H_{i-1}}, \tag{42}$$

where

$$H_{i-1} = \int_0^{A_{cr}} p(A_{i-1}, t_{i-1}) dA_{i-1} \tag{43}$$

and

$$Q_{i-1,i} = \int_0^{A_{cr}} \left[\int_{A_{cr}}^{\infty} p(A_i, t_i \mid A_{i-1}, t_{i-1}) \, dA_i \right] p(A_{i-1}, t_{i-1}) \, dA_{i-1} \tag{44}$$

with $p(A_{i-1}, t_{i-1})$ defined in Eq. (24). Next, considering also Eqs. (35), (43) and (44) can be reformulated respectively as follows

$$H_{i-1} = 1 - \exp\left[-\frac{A_{cr}^2}{2c(t_{i-1})} \right] \tag{45}$$

and

$$Q_{i-1,i} = \int_0^{A_{cr}} \left\{ \int_{A_{cr}}^{\infty} \left[p_{tr}(A_i, t_i \mid A_{i-1}, t_{i-1}) \right.\right.$$
$$\left.\left. + R(t_i, t_{i-1}) \delta(A_i - A_\infty) \right] dA_i \right\} p(A_{i-1}, t_{i-1}) dA_{i-1} \tag{46}$$

Next, by considering the properties of the Dirac delta function and substituting Eqs. (39) and (45), (46) can be simplified into the form

$$Q_{i-1,i} = H_{i-1} - \int_0^{A_{cr}} \int_0^{A_{cr}} p_{tr}(A_i, t_i | A_{i-1}, t_{i-1}) p(A_{i-1}, t_{i-1}) dA_i dA_{i-1} \tag{47}$$

Assuming that $\omega_{\text{eq,B}}$ varies slowly with time, it can be approximated as a constant within the small time interval $[t_{i-1}, t_i]$, such that $\omega_{\text{eq,B}}(t) = \omega_{\text{eq,B}}(t_{i-1})$ for all $t \in [t_{i-1}, t_i]$. Similarly, $S_w(\omega, t)$ is also treated as constant over the interval $[t_{i-1}, t_i]$ due to the slow time-varying behavior of the EPS [27]. Under these assumptions, and by defining $\tau_i = t_i - t_{i-1}$, a first-order Taylor expansion about $\tau_i = 0$ can then be applied to discretize the time-varying coefficients of Eqs. (37) and (38) into

$$c(t_{i-1}, t_i) = \frac{\pi \lambda^2 S_w \left[\omega_{\text{eq,B}}(t_{i-1}), t_{i-1} \right]}{\omega_{\text{eq,B}}^2(t_{i-1})} \tau_i \tag{48}$$

and

$$h(t_{i-1}, t_i) = A_{i-1} \sqrt{1 - \beta_{eq,B}(t_{i-1}) \tau_i} \tag{49}$$

respectively. Notably, Eqs. (41)–(43) and (47)–(49) can be used for the computation of the time-varying seakeeping probability $P_S(t)$ of a ship rolling in beam seas subjected to non-white sea-wave excitation. Additionally, the consideration of Eqs. (37) and (48) and the application of a first-order Taylor expansion for the time-varying coefficient $c(t_i)$ around the point $t = t_{i-1}$ yield

$$c(t_i) = c(t_{i-1}, t_i) + c(t_{i-1})(1 - \beta_{\text{eq,B}}(t_{i-1}) \tau_i) \tag{50}$$

with Eq. (50) being rearranged into

$$c(t_{i-1}, t_i) = c(t_i)(1 - r_i^2) \tag{51}$$

where the introduced parameter r_i^2 is defined as

$$r_i^2 = \frac{c(t_{i-1})}{c(t_i)} (1 - \beta_{\text{eq,B}}(t_{i-1}) \tau_i) \tag{52}$$

and serves as a measure of the correlation between the random variables A_{i-1} and A_i.

2.5. Discussion on attributes of the proposed stochastic roll dynamics method

This section examines several key attributes of the proposed stochastic roll dynamics framework, with emphasis on its main contributions, practical advantages, and current limitations. Overall, the methodology provides a versatile and computationally efficient tool for time-dependent assessment of seakeeping performance and capsizing risk in ship–sea systems governed by complex nonlinear roll dynamics.

A principal contribution of the approach is its ability to represent, within a single physically consistent formulation, roll systems exhibiting both softening and hardening restoring behavior together with nonlinear hydrodynamic damping. Through equivalent linearization based on the pseudo-harmonic assumption, the method accommodates amplitude-dependent as well as time-dependent variations in the effective natural frequency and damping while preserving analytical tractability and offering a probabilistic insight into the ship–sea system dynamics. A further key contribution is the adoption of a tailored Rayleigh-type representation for the rolling angle amplitude statistics, which enables a clear probabilistic separation between bounded and unbounded responses; this feature is particularly important for capsizing-related assessments in the presence of negative-stiffness effects. On this basis, the method yields explicit time-dependent seakeeping probabilities, providing reliability-oriented insight into ship performance under non-stationary and irregular sea environments. Importantly, the framework places limited restrictions on the excitation model, requiring only Gaussianity of the input, and is therefore applicable to a wide range of realistic sea-wave scenarios, including evolutionary processes with time-varying intensity and frequency content.

In the context of early-stage performance-based ship design, the framework is particularly attractive for rapid screening of candidate designs under operational sea states, where extensive Monte Carlo simulation may be prohibitive. Nevertheless, it should be noted that while the integration of stochastic averaging and equivalent statistical linearization is highly effective for lightly damped or moderately nonlinear systems, its accuracy may degrade in heavily damped configurations or in the presence of strong nonlinearities. In summary, the method offers a flexible, physically interpretable, and computationally tractable route for time-dependent seakeeping and capsizing risk estimation under non-stationary and irregular sea-wave excitation, firmly rooted in the practical needs of naval engineering.

3. Numerical application

This section presents the numerical results of the vessel seakeeping performance assessment method based on the mathematical framework established in Sections 2.1–2.4. Variations in the input significant wave height H_s as well as in the system weighting factors ε_1, ε_2, and ε_3, are considered. The results are validated against pertinent MCS data

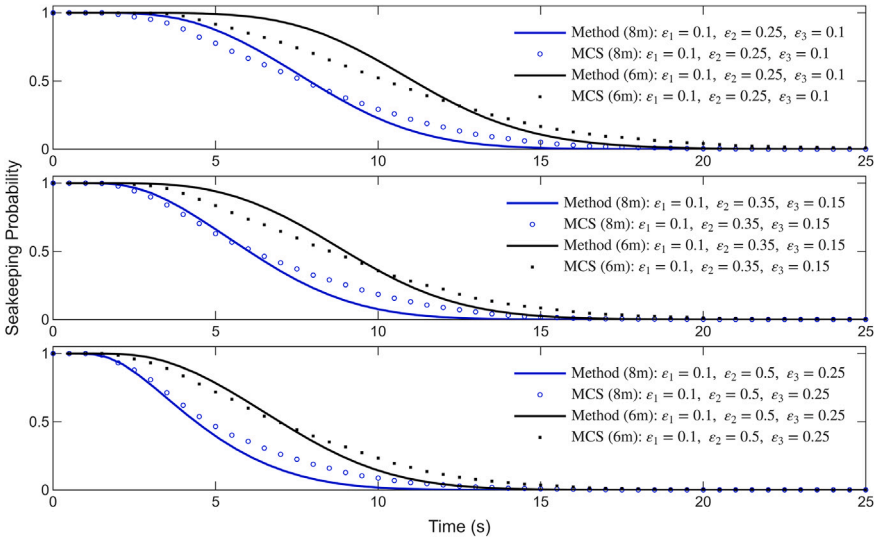

Fig. 4. Seakeeping probability of a nonlinear ship rolling system under evolutionary sea-wave excitation for nominal wave heights $H_s = 6$ m and $H_s = 8$ m, with $b_N = 0.042$; comparisons with MCS data (5000 realizations).

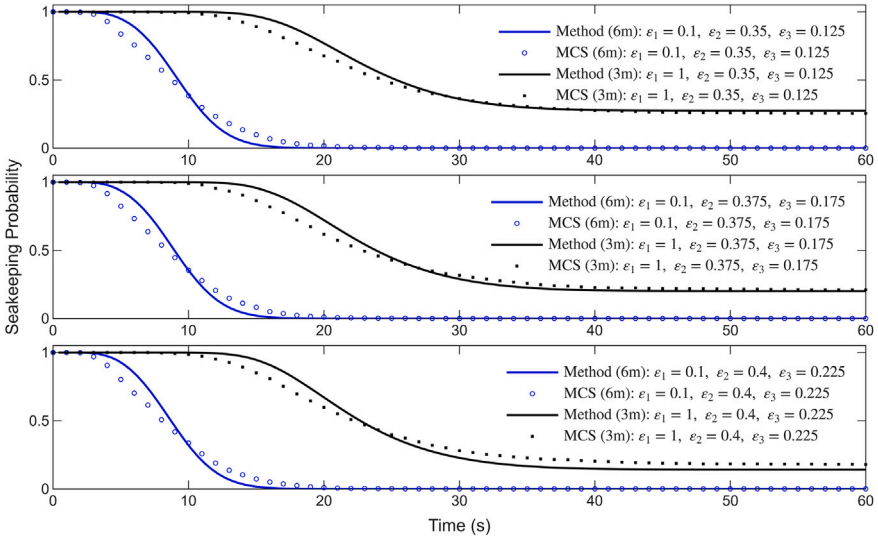

Fig. 5. Seakeeping probability of a nonlinear ship rolling system under evolutionary sea-wave excitation for nominal wave heights $H_s = 3$ m and $H_s = 6$ m, with $b_N = 0.25$; comparisons with MCS data (5000 realizations).

to demonstrate the efficiency and reliability of the proposed approach. For all wave height scenarios, the hydrodynamic excitation is characterized by a peak period of $T_p = 15.5$ s. The ship rolling parameters are, $\phi_v = 0.96$rad, $A_{\phi v} = 0.67\,\text{m}\cdot\text{rad}$, $GM = 3$ m, $I_{xx} = 1\times10^8$ kg·m^2, $\delta I_{xx} = 0.2 I_{xx}$, $B_L = 5\times10^6$N·m·s, $B_N = 5\times10^6$N·m·s^2 and $\Delta = 1\times10^8$ N (e.g., [48,49]). Fig. 4 presents the time-dependent seakeeping probability for a ship subjected to significant sea-wave heights H_s of 6 m and 8 m, where the nonlinear damping is held at $b_N = 0.042$, the nonlinear damping weighing factor is fixed at $\varepsilon_1 = 0.1$, and variations in ε_2 and ε_3 are introduced with respect to the restoring force characteristics. The MCS results presented alongside the semi-analytical predictions reveal a satisfactory degree of accuracy. Additionally, Fig. 5 presents a complementary case study associated with a higher nonlinear damping coefficient ($b_N = 0.25$), considering as well variations across the weighting factors ε_1, ε_2, and ε_3. This case also explores different sea states with significant wave heights H_s equal to 3 m and 6 m, capturing scenarios in which non-zero seakeeping probability is observed. To improve the accuracy of the analysis under stronger excitations that induce pronounced nonlinear behavior, particularly when the equivalent natural period $T_{eq}(t)$ marches toward higher values, an adaptive time discretization step of $d_T = 0.1$ is prioritized. This preserves the validity of the assumption that the seakeeping probability remains approximately constant over each time-interval (e.g., [13,27]). For all cases, the performance of the proposed methodology is assessed by direct comparison with MCS results based on 5000 realizations (e.g., [12,14]), demonstrating its capability and robustness in quantifying vessel seakeeping ability under sea-wave stochastic excitation. More precisely, the spectral representation method outlined in [50] is employed to create the ensemble of realizations, compatible with the reference seed power spectrum corresponding to a specific nominal wave height for the induced hydrodynamic excitation of Eq. (1). The corresponding system response is then obtained through numerical integration of the governing equation of nonlinear ship motion Eq. (9).

It can be noted that at any given time instant, the seakeeping probability associated with the lower nominal wave height condition (black line) is consistently higher than that corresponding to the higher wave

height (blue line). This observation aligns with engineering intuition, as lower wave heights impart reduced excitation energy to the system, thereby decreasing the likelihood of capsizing and improving the vessel's seakeeping performance. The proposed methodology demonstrates a satisfactory degree of agreement with the MCS benchmark across a range of values for the considered weighting factors ϵ. Its consistent performance under varying wave heights further underscores the robustness of the approach in accommodating different excitation characteristics, rendering it well-suited for application across diverse and representative sea states. In the presented case studies, specific values of ϵ_2 and ϵ_3 in the righting arm (GZ) curve were selected to ensure that the hardening effects associated with the fifth-order term remain of lower magnitude compared to the softening effects of the third-order term. This choice is further supported by the nature of the restoring coefficients m_3 and m_5, where m_3 is considerably higher in magnitude than m_5, reinforcing the dominance of softening behavior initially. The condition of $\epsilon_2 > \epsilon_3$ enables a balanced yet flexible representation of softening and hardening effects, fully consistent with ship roll modeling practices found in the broader relevant literature (e.g., Taylan [36]). Mild to soft hardening behavior may also arise from appendages such as bilge keels or stabilizing fins mounted on the sides of large vessels. Bilge keels, functioning as passive devices, primarily enhance hydrodynamic damping but can introduce a limited restoring effect at large roll angles, thereby contributing marginally to hardening nonlinearity. In contrast, stabilizer fins, particularly active systems can generate additional restoring moments that increase nonlinearly with roll angle, especially at higher amplitudes. These physical effects are mathematically reflected as a positive fifth-order term in the restoring moment polynomial. Nevertheless, the magnitude of this hardening component typically remains much smaller than that of the third-order (softening) term, in line with the dominant softening behavior observed in conventional ship designs. While this formulation provides a meaningful means of assessing capsizing probability within the proposed seakeeping assessment framework, a key strength is its flexibility in modeling nonlinear ship roll dynamics. By employing a fifth-order polynomial for the GZ curve and introducing tailored weighting factors, the method can represent both softening and hardening restoring behaviors, as well as nonlinear hydrodynamic damping effects. This dual consideration of nonlinearity in both damping and restoring force increases model complexity, but significantly enhances its ability to capture the range of relevant ship roll dynamics.

4. Concluding remarks

This study proposes an efficient semi-analytical methodology for assessing the seakeeping ability and the capsizing risk of ships exhibiting nonlinear rolling dynamics under realistic, non-white sea-wave excitations. The modeling is grounded in a comprehensive and physically consistent nonlinear formulation, integrating both softening and hardening restoring moment characteristics alongside nonlinear hydrodynamic damping, and is driven by evolutionary stochastic wave loads representative of complex maritime environments. Central to the approach is a refined blend of stochastic averaging and statistical linearization techniques, which enable computationally efficient and time-dependent estimation of seakeeping probabilities. This methodological synergy allows for rigorous treatment of both bounded and unbounded roll responses, associated with negative stiffness values, through an appropriately introduced tailored, non-stationary response amplitude probability density function.

A key feature of the framework is its robust capability to capture the effects of stochastic sea-wave excitations with time-varying intensity and frequency content, ensuring the method faithfully reflects the dynamic and irregular nature of open-sea conditions. The approach demonstrates significant computational efficiency and delivers reliable estimates of seakeeping ability, as validated through comparison with benchmark Monte Carlo simulation results. By advancing the theoretical and computational modeling of nonlinear ship rolling dynamics, this study contributes a practical, scalable, and performance-based tool for safety evaluation and operational planning, particularly in early design stages where full-scale simulations are often impractical.

CRediT authorship contribution statement

Ioannis P. Mitseas: Writing – review & editing, Writing – original draft, Visualization, Supervision, Software, Project administration, Methodology, Conceptualization. **Omar Danisworo:** Writing – review & editing, Visualization, Software.

Declaration of competing interest

The authors declare that they have no known competing financial interests or personal relationships that could have appeared to influence the work reported in this paper.

Data availability

Data will be made available on request.

References

[1] Arnold L, Chueshov I, Ochs G. Stability and capsizing of ships in random sea-a survey. Nonlinear Dyn 2004;36:135–79.
[2] Belenky VL, Sevastianov NB. Stability and safety of ships: risk of capsizing. The Society of Naval Architects and Marine Engineers; 2007.
[3] Spyrou K, Thompson J. The nonlinear dynamics of ship motions: a field overview and some recent developments. Philos Trans R Soc A Math Phys Eng Sci 2000;358:1735–60.
[4] Chai W, Naess A, Leira BJ. Stochastic nonlinear ship rolling in random beam seas by the path integration method. Probabilist Eng Mech 2016;44:43–52.
[5] Senjanović I, Grubisić R. Coupled horizontal and torsional vibration of a ship hull with large hatch openings. Comput Struct 1991;41(2):213–26.
[6] IMO, London, UK. International code on intact stability. IMO London, UK; 2008.
[7] To CWS, Chen Z. First passage time of nonlinear ship rolling in narrow band non-stationary random seas. J Sound Vib 2008;309:197–209.
[8] Falzarano JM, Su Z, Jamnongpipatkul A, Somayajula A. Solving the problem of nonlinear ship roll motion using stochastic dynamics. Cham: Springer International Publishing; 2019.
[9] Senjanović I, Ciprić G, Parunov J. Survival analysis of fishing vessels rolling in rough seas. Philos Trans R Soc A Math Phys Eng Sci 2000;358:1943–65.
[10] American Bureau of Shipping. Guide for fatigue assessment of offshore structures. Houston, TX: American Bureau of Shipping; 2020.
[11] IEC 61400-3-1:2019 Wind energy generation systems – Part 3-1: Design requirements for fixed offshore wind turbines. International Electrotechnical Commission; 2019.
[12] Kougioumtzoglou IA, Spanos PD. Stochastic response analysis of the softening duffing oscillator and ship capsizing probability determination via a numerical path integral approach. Probabilist Eng Mech 2014;35:67–74.
[13] Mitseas IP, Beer M. First-excursion stochastic incremental dynamics methodology for hysteretic structural systems subject to seismic excitation. Comput Struct 2021;242:106359.
[14] Mitseas IP, Ni P, Fragkoulis VC, Beer M. Survival probability surfaces of hysteretic fractional order structures exposed to non-stationary code-compliant stochastic seismic excitation. Eng Struct 2024;318:118755.
[15] Schueller G, Jensen H, Holicky L. Computational methods in stochastic mechanics and reliability analysis. Arch Comput Methods Eng 2004;11:113–90.
[16] Ni P, Fragkoulis V, Kong F, Mitseas I, Beer M. Non-stationary response of nonlinear systems with singular parameter matrices subject to combined deterministic and stochastic excitation. Mech Syst Signal Process 2023;188:110009.
[17] Kougioumtzoglou IA, Ni P, Mitseas IP, Fragkoulis VC, Beer M. An approximate stochastic dynamics approach for design spectrum-based response analysis of nonlinear oscillators with fractional derivative elements. Int J Non Linear Mech 2022;146:104178.
[18] Jerez D, Fragkoulis V, Ni P, Mitseas I, Valdebenito MA, Faes MG, Beer M. Operator norm-based determination of failure probability of nonlinear oscillators with fractional derivative elements subject to imprecise stationary Gaussian loads. Mech Syst Signal Process 2024;208:111043.
[19] MSC, IMO, London, UK. 1/Circ. 1627 interim guidelines on the second generation intact stability criteria; 2020.
[20] Barbato M, Conte JP. First-passage reliability analysis of nonlinear systems under nonstationary random excitation. Struct Saf 2001;23(4):355–74.
[21] Mitseas IP, Kougioumtzoglou IA, Spanos PD, Beer M. Nonlinear MDOF structural system survival probability determination subject to evolutionary stochastic excitation. Stroj Vestn J Mech Eng 2016;62(7–8):440–51.
[22] Roberts J, Vasta M. Markov modelling and stochastic identification for nonlinear ship rolling in random waves. Philos Trans R Soc A Math Phys Eng Sci 2000;358:1917–41.
[23] Roberts J, Dunne J, Debonos A. Stochastic estimation methods for non-linear ship roll motion. Probabilist Eng Mech 1994;9(1):83–93.

[24] Li J. Probability density evolution method: background, significance and recent developments. Probabilist Eng Mech 2016;44:111–7.
[25] Xu J, Chen J, Li J. Probability density evolution analysis of engineering structures via cubature points. Comput Mech 2012;50:135–56.
[26] Náprstek J, Král R. Finite element method analysis of fokker–plank equation in stationary and evolutionary versions. Adv Eng Softw 2014;72:28–38.
[27] Kougioumtzoglou IA, Zhang Y, Beer M. Softening duffing oscillator reliability assessment subject to evolutionary stochastic excitation. ASCE-ASME J Risk Uncertain Eng Syst Part A Civil Eng 2015;2(2):04015002.
[28] Ni P, Mitseas IP, Fragkoulis VC, Beer M. Spectral incremental dynamic methodology for nonlinear structural systems endowed with fractional derivative elements subjected to fully non-stationary stochastic excitation. Struct Saf 2024;111:102525.
[29] Ni P, Fragkoulis VC, Kong F, Mitseas IP, Beer M. Response determination of nonlinear systems with singular matrices subject to combined stochastic and deterministic excitations. ASCE ASME J Risk Uncertain Eng Syst Part A Civil Eng 2021;7(4):04021049.
[30] Mitseas IP, Beer M. Modal decomposition method for response spectrum based analysis of nonlinear and non-classically damped systems. Mech Syst Signal Process 2019;131:469–85.
[31] Spanos PD, Kougioumtzoglou IA, dos Santos KR, Beck AT. Stochastic averaging of nonlinear oscillators: hilbert transform perspective. J Eng Mech 2018;144(2):04017173.
[32] Náprstek J, Fischer C. Semi-analytical stochastic analysis of the generalized van der pol system. Appl Comput Mech 2018;12(1).
[33] Moshchuk N, Ibrahim R, Khasminskii R, Chow P. Asymptotic expansion of ship capsizing in random sea waves—i. first-order approximation. Int J Non Linear Mech 1995;30(5):727–40.
[34] Ren Z, Xu W, Wang D. Dynamic and first passage analysis of ship roll motion with inelastic impacts via path integration method. Nonlinear Dyn 2019;97:391–402.
[35] Malara G, Spanos PD, Arena F. Maximum roll angle estimation of a ship in confused sea waves via a quasi-deterministic approach. Probabilist Eng Mech 2014;35:75–81.
[36] Taylan M. The effect of nonlinear damping and restoring in ship rolling. Ocean Eng 2000;27(9):921–32.
[37] Jiang C, Troesch AW, Shaw SW. Capsize criteria for ship models with memory-dependent hydrodynamics and random excitation. Philos Trans R Soc A Math Phys Eng Sci 2000;358:1761–91.
[38] Hasselmann K, Barnett T, Bouws E, Carlson H, Cartwright D, Enke K, Ewing J, Gienapp H, Hasselmann D, Kruseman P, Meerburg A, Müller P, Olbers D, Richter K, Sell W, Walden H. Measurements of wind-wave growth and swell decay during the joint North Sea Wave Project (JONSWAP), Tech. Rep. 12, dtsch. Hydrogr. Z. Suppl.A8 (1973).
[39] Branlard E. Generation of time series from a spectrum: generation of wave times series from the JONSWAP spectrum, Tech. rep. Risø DTU, National Laboratory for Sustainable Energy; 2010.
[40] Wright J, Marshfield W. Ship roll response and capsize behaviour in beam seas. Trans R Inst Nav Archit 1979;122:129–48.
[41] Chen J, Yang J, Shen K, Zheng Z, Chang Z. Stochastic dynamic analysis of rolling ship in random wave condition by using finite element method. Ocean Eng 2022;250:110973.
[42] Kougioumtzoglou IA, Spanos PD. An approximate approach for nonlinear system response determination under evolutionary stochastic excitation. Curr Sci 2009;97:1203–11.
[43] Roberts JB, Spanos PD. Random vibration and statistical linearization. Courier Corporation; 2003.
[44] Spanos PD, Lutes LD. Probability of response to evolutionary process. J Eng Mech Div 1980;106(2):213–24.
[45] Mitseas IP, Beer M. Fragility analysis of nonproportionally damped inelastic MDOF structural systems exposed to stochastic seismic excitation. Comput Struct 2020;226:106129.
[46] Spanos PD, Solomos GP. Markov approximation to transient vibration. J Eng Mech 1983;109(4):1134–50.
[47] Roberts JB, Spanos PD. Stochastic averaging: an approximate method of solving random vibration problems. Int J Non Linear Mech 1986;21(2):111–34.
[48] Surendran S, Reddy JVR. Numerical simulation of ship stability for dynamic environment. Ocean Eng 2003;30(10):1305–17.
[49] Kianejad S, Enshaei H, Duffy J, Ansarifard N. Prediction of a ship roll added mass moment of inertia using numerical simulation. Ocean Eng 2019;173:77–89.
[50] Shinozuka M, Deodatis G. Simulation of stochastic processes by spectral representation. ASME. Appl Mech Rev 1995;44(4):191–204.